Supplementary Online Material for:

Binding and Translocation of Termination Factor Rho Studied at the Single-Molecule Level

Daniel J. Koslover[1†], Furqan M. Fazal[2†], Rachel A. Mooney[4], Robert Landick[4], Steven M. Block[2,3*]

[1]*Biophysics Program, Stanford University, Stanford, CA 94305, USA.*
[2]*Department of Applied Physics, Stanford University, Stanford, CA 94305, USA*
[3]*Department of Biology, Stanford University, Stanford, CA 94305, USA*
[4]*Department of Biochemistry, University of Wisconsin-Madison, Madison, WI 53706, USA*

[†]D.J.K and F.M.F. contributed equally to this work.
[*]*Corresponding author*. Department of Biology, Stanford University, Stanford, CA 94305, USA. E-mail address: sblock@stanford.edu

Supplementary Results and Discussion

Rho Terminates RNAP with Close to 50% Efficiency

The λtR1 terminator was inserted into the *rpoB* gene of plasmid pRL732,[1] downstream of the T7A1 promoter. Rho-dependent termination was assayed in vitro under both single-molecule and bulk conditions in the same elongation buffer (Experimental Procedures). We observed a termination efficiency of ~60% in a single-molecule assay (9 of 15 records terminating, 5 pN hindering load, 5 nM Rho) that was based on a previously described experimental geometry,[2] with RNAP attached to one bead via a biotin-avidin linkage, and the downstream end of the DNA template attached to a second bead via a digoxigenin-antidigoxigenin linkage. A termination efficiency of ~45% was observed with the same template when assayed by a polyacrylamide gel (20 nM Rho). Termination was not observed under either condition in the absence of Rho.

Initiation of Rho Translocation May Require an Additional Step after Ring Closure

Rho complexes studied in the presence of ATP could be separated into two distinct populations: those that generated translocation rips, which presumably moved along RNA, and those that generated only primary and secondary rips, which presumably failed to move (the latter population was also reproduced in the presence of AMP-PNP). The force required to release the RNA associated with translocations rips in complexes that moved (16.2 ± 0.8 pN; N = 43) was the same, within error, as the force associated with secondary rips in complexes that did not move (14.7 ± 0.7 pN; N = 49). If Rho were to first bind RNA at both primary and secondary sites, and subsequently transition from the open form to the closed form prior to translocation, one might expect the force required to release RNA from the open form to be significantly lower than from the closed form, where the RNA is threaded through the middle of the complex and therefore topologically constrained. The similarity in the release forces therefore suggests that the Rho complexes sampled in these experiments is in the same conformational states before and after translocation (both open, or both closed). The simplest explanation, which we favor, is that Rho transitions to the closed form upon binding RNA at its secondary site prior to translocation, and therefore that data acquired on secondary and translocation rips reflect the release of RNA from complexes that had already transitioned to a closed form in all instances. Because we observed a population of complexes that bound to both primary and secondary sites in the presence of ATP but did not translocate, it seems likely that Rho undergoes an additional transition following closure of the enzyme in order to become competent for translocation. The alternative possibility, which cannot be distinguished by these data, is that Rho complexes that fail to translocate remain in an open state, and complexes that successfully translocate transition back to this same open state after movement ceases.

Supplementary Experimental Procedures

Sequence elements introduced into the pALB3 template:

1. Insert with λtR1 terminator (129 nt)

ATAACCCCGCTCTTACACATTCCAGCCCTGAAAAAGGGCATCAAATTAAACCACACC
TATGGTGTATGCATTTATTTGCATACATTCAATCAATTGTTATCTAAGGAAATACTTA
CATATGGTTCGTGC

2. Insert with λtR1-*rut* site (68 nt)

ATAACCCCGCTCTTACACATTCCAGCCCTGAAAAAGGGCATCAAATTAAACCACACC
TATGGTGTATG

3. Insert with λtR1-*rut* site, *boxB*-deletion mutant (53 nt)

ATAACCCCGCTCTTACACATTCCAATCAAATTAAACCACACCTATGGTGTATG

4. Insert with λtR1-*rut* site with additional upstream sequence derived from *cro* (107 nt)

ATAAAGCCCTTCCCGAGTAACAAAAAAACAACAGCATAAATAACCCCGCTCTTACA
CATTCCAGCCCTGAAAAAGGGCATCAAATTAAACCACACCTATGGTGTATG

(Note: Nucleotides 2–39 in this sequence are from the *cro* gene. The first nucleotide was mutated to A to minimize any secondary structure formation in the transcribed RNA, as predicted by mfold.[3])

Sequences were inserted 36 bp downstream of the T7A1 promoter in the pALB3-DNA template at a BstEII digestion site. For single-molecule experiments, DNA templates were amplified from plasmids by PCR using a downstream primer with a 3′-biotin moiety that ultimately formed part of the biotin-streptavidin roadblock. The roadblock was constructed by incubating the PCR product with 20-fold excess streptavidin (ProZyme) for 30 min at room temperature (21.5 ± 0.5 ˚C) followed by addition of 1000-fold excess biotin to bind any residual streptavidin. After incubating for an additional 30 min, the DNA was purified (QIAquick PCR Purification Kit, Qiagen).

To prepare stalled elongation complexes (ECs), biotinylated RNAP was initiated at 37 C at the T7A1 promoter in the presence of 2.5 μM ATP, CTP, and GTP and allowed to transcribe the first 29 nt of the template.[1] ECs were then purified from free nucleotides on a Sepharose column (GE Healthcare) and stored at –80 ˚C. Aliquots of frozen ECs were thawed for experiments and stored at 4 ˚C for up to 3 days. Carboxyl-functionalized polystyrene beads (0.60 μm and 0.73 μm diameter; Bangs Laboratories) were functionalized with avidin as described.[1] Beads were washed in wash buffer (50 mM HEPES [pH 8.0], 130 mM KCl, 5 mM $MgCl_2$, 0.1 mM EDTA, 0.1 mM DTT) and sonicated prior to use. Rho was stored at –80 ˚C in 50% glycerol and 50% wash buffer at a concentration of 1.56 μM (assuming hexamers). On the day of the experiment, Rho was diluted to a final concentration of 20 nM in elongation buffer (Experimental Procedures).

To make the 3,057-bp dsDNA handle, autosticky PCR of the M13mp18 plasmid by rTth DNA Polymerase, XL (Applied Biosystems) was performed. One primer was 25-nt long and carried a 5′ biotin while the other had a 25-nt hybridization segment followed by a single abasic site and a 25-nt overhang.[4]

All primers and oligomers were purchased (Integrated DNA Technologies) and all templates were sequenced (Sequetech). The 20-nt-blocking oligomer was complementary to nucleotides 11 through 30 of the transcript downstream of the *rut* site. Concentrations of DNA, glucose oxidase, and catalase were measured on a Nanodrop 2000 Spectrophotometer (Thermo Scientific). NTPs and AMP-PNP were purchased (Roche Molecular Biochemicals). All gel-based experiments were carried out at room temperature.

Supplementary References

1. Neuman, K. C., Abbondanzieri, E. A., Landick, R., Gelles, J. & Block, S. M. (2003). Ubiquitous transcriptional pausing is independent of RNA polymerase backtracking. *Cell* **115**, 437-47.

2. Larson, M. H., Greenleaf, W. J., Landick, R. & Block, S. M. (2008). Applied force reveals mechanistic and energetic details of transcription termination. *Cell* **132**, 971-82.

3. Zuker, M. (2003). Mfold web server for nucleic acid folding and hybridization prediction. *Nucleic Acids Res* **31**, 3406-15.

4. Gal, J., Schnell, R., Szekeres, S. & Kalman, M. (1999). Directional cloning of native PCR products with preformed sticky ends (autosticky PCR). *Mol Gen Genet* **260**, 569-73.

Supplementary Figure Legends

Figure S1. *boxB* Hairpin Unfolds when Rho Binds *rut* Site

Histogram of the rip sizes for Rho bound to template RB30 with a *boxB* deletion (7 molecules; $N = 67$). Inset: schematic of the construct, using the same color scheme as Fig. 3a. A single population of unbinding rips is centered at 27 ± 1 nm, and has the identical size (within statistical error) as the 28 nm primary rips observed when *boxB* was present (Fig. 3). No secondary rips (45 nm) were observed.

Figure S2. Predictions for Intermediate Rho Unbinding Rips

Combining our unbinding results with structural data, we computed the sizes of sub-rips expected for four potential intermediate states during the release of RNA from the Rho complex. Here, we consider a scenario where RNA dissociates from the six primary domains sites in a two-step process, with the first step corresponding to release from one, two, three, or four sites. (An intermediate where RNA is released from five sites was not considered, since it cannot be distinguished experimentally from the complete release of RNA.) The size of the second sub-rip

was calculated using $r = 0.59N - d$, where r is the sub-rip size (in nm), N is the number of nucleotides bound to Rho, and d is the distance (in nm) separating the initial and final attachment points of the RNA. The value of d was determined using the locations of dinucleotides fragments found in the open crystal structure (PDB ID: 1PVO), and measured 6.59 ± 0.30 nm (a), 6.90 ± 0.04 nm (b), 5.70 ± 0.15 nm (c), and 3.02 ± 0.04 nm (d). To obtain N, we multiplied the number of nucleotides predicted to bind all primary domains in a lock-washer configuration, 56.6 ± 1.6, by the factors 4/5 (a), 3/5 (b), 2/5 (c), and 1/5 (d). The expected size of the first sub-rip was obtained by subtracting the computed value of the second rip from the primary rip size of 28.0 nm.

Figure S3. Intermediates in Translocation Rips

(a–c) Representative FECs, depicting examples of the different types of translocation rips. FECs without Rho-dependent rips (green) are shown for comparison.

(a) 44% of translocation rips (blue trace) occurred as a single event with no intermediate.

(b) 23% of translocation rips (red trace) displayed two sub-rips. The size of the first sub-rip was proportional to the length of the template (~44 nm for RB75, ~83 nm for RB150); the size of the second sub-rip was ~28 nm.

(c) 33% of translocation rips (black trace) displayed sub-rips of variable size that could not be associated with any specific intermediate structure.

(c') A model in which non-specific interactions formed within the loop of RNA produced during tethered tracking (e.g., RNA secondary structure formation) give rise to the variable sub-rips in experimental records. In such a scenario, sub-rips can occur only after an initial release of at least

17 nm (after RNA has been released from the Rho secondary site, but prior to release from any primary sites) and the RNA loop experiences the applied force.

Table S1. Summary of data for all five templates studied, under the nucleotide conditions indicated

The measured sizes of primary, secondary, and translocation rips are shown. Integers in parentheses denote the associated numbers of rip events.

Figure S1

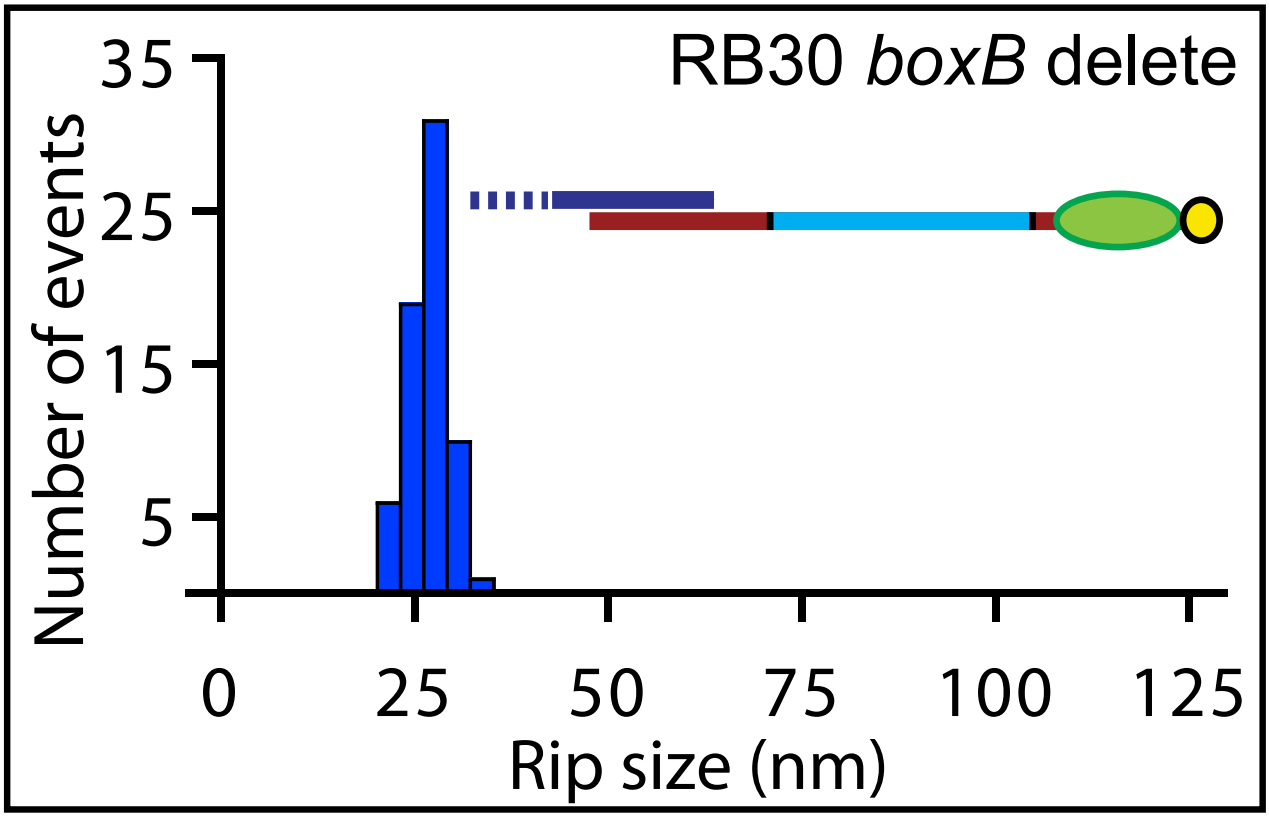
RB30 boxB delete
Number of events
35
25
15
5
0
25
50
75
100
125
Rip size (nm)

Figure S2

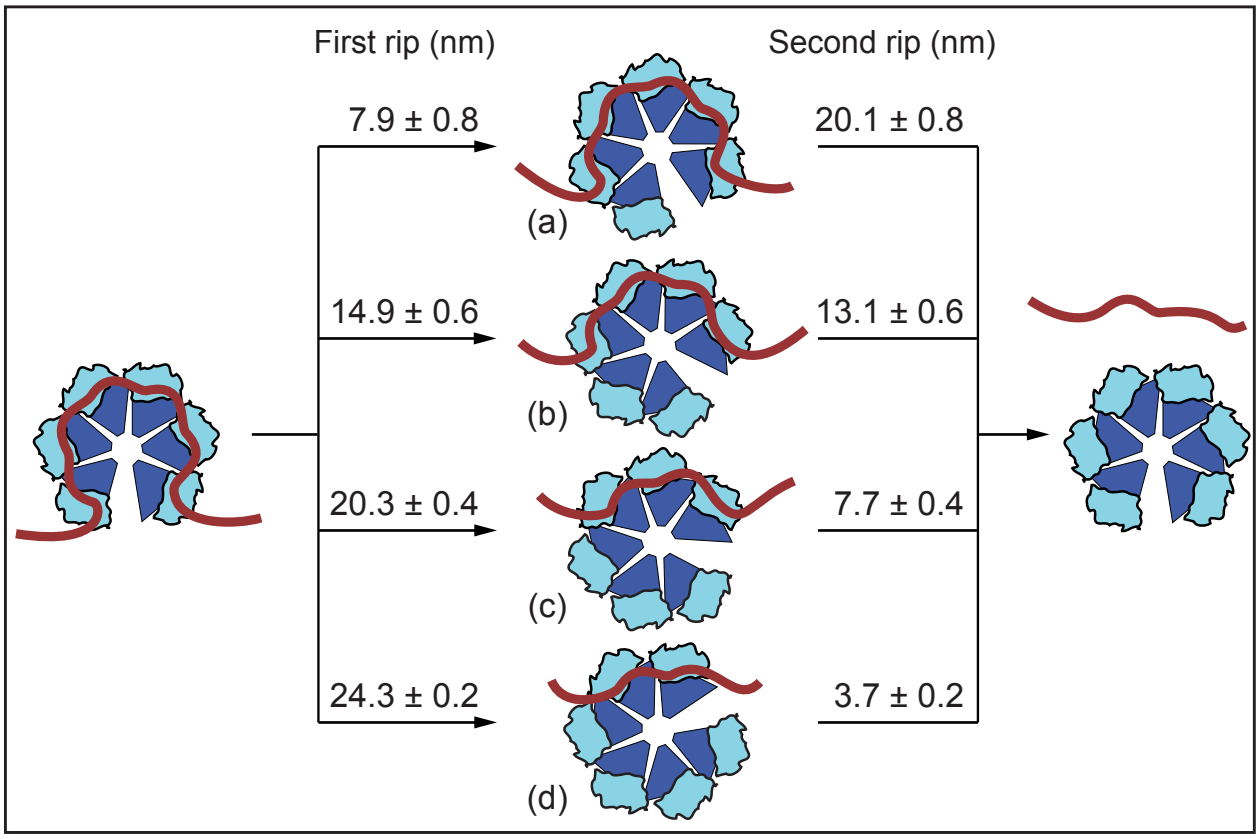
First rip (nm)
Second rip (nm)
7.9 ± 0.8
20.1 ± 0.8
(a)
14.9 ± 0.6
13.1 ± 0.6
(b)
20.3 ± 0.4
7.7 ± 0.4
(c)
24.3 ± 0.2
3.7 ± 0.2
(d)

Figure S3

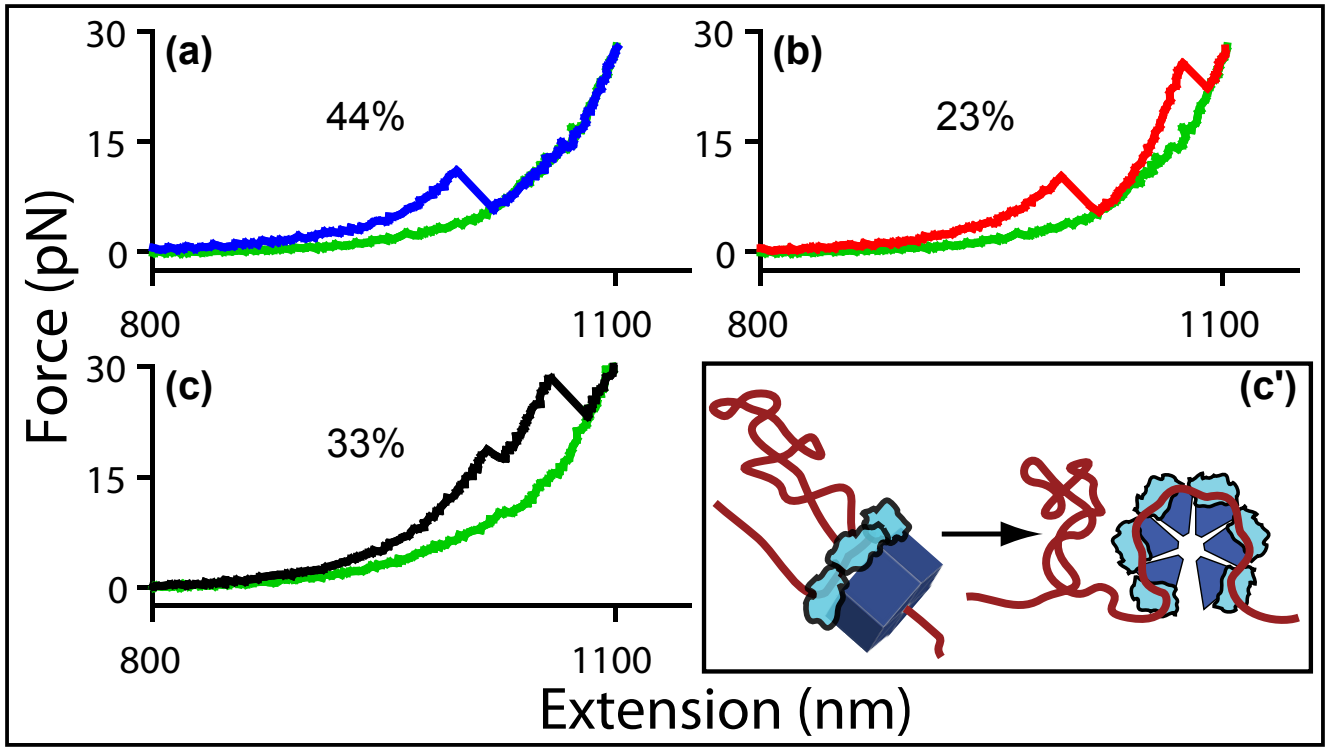

Table S1

Construct	Condition	Number of Molecules	1 Primary (nm)	1 Secondary (nm)	2 Primary (nm)	3 Primary (nm)	Translocation (nm)
RB30	AMP-PNP	8 (33)	28.5 ± 1.0 (24)	46.4 ± 1.1 (9)	-----	-----	-----
RB30	ATP	8 (37)	29.6 ± 1.1 (21)	46.3 ± 0.8 (16)	-----	-----	-----
RB75	AMP-PNP	22 (65)	28.4 ± 0.6 (44)	44.8 ± 0.5 (14)	57.3 ± 1.3 (7)	-----	-----
RB75	ATP	33 (96)	27.8 ± 0.5 (62)	43.9 ± 0.5 (12)	56.8 ± 1.0 (12)	-----	72.7 ± 1.5 (10)
RB75	ATP w/ blocking oligo	43 (98)	27.7 ± 0.4 (57)	45.3 ± 0.7 (29)	57.5 (1)	-----	70.7 ± 1.5 (11)
RB150	AMP-PNP	17 (54)	26.8 ± 1.0 (6)	------	54.7 ± 1.4 (25)	83.7 ± 1.1 (23)	-----
RB150	ATP	37 (114)	29.7 ± 0.8 (20)	-----	55.6 ± 1.0 (41)	83.9 ± 0.9 (35)	111.0 ± 1.3 (18)
RB30 *boxB* delete	ATP	7 (67)	26.5 ± 0.3 (67)	-----	-----	-----	-----
RB75 w/ additional 39 nt upstream	ATP	27 (60)	29.4 ± 0.6 (24)	44.1 ± 1.1 (8)	56.1 ± 0.5 (24)	-----	69.5 ± 2.4 (4)